POLITECNICO DI TORINO
Repository ISTITUZIONALE

A New Analytical Solution for Calculating Rock Block Volume

Original
A New Analytical Solution for Calculating Rock Block Volume / Umili, G., Carriero, M.T., Taboni, B., Migliazza, M., Ferrero, A.M.. - In: ROCK MECHANICS AND ROCK ENGINEERING. - ISSN 0723-2632. - 57:5(2024), pp. 3109-3120. [10.1007/s00603-023-03728-y]

Availability:
This version is available at: 11583/2989482 since: 2024-06-13T08:23:27Z

Publisher:
Springer

Published
DOI:10.1007/s00603-023-03728-y

Terms of use:

This article is made available under terms and conditions as specified in the corresponding bibliographic description in the repository

Publisher copyright

(Article begins on next page)

27 November 2026

Rock Mechanics and Rock Engineering (2024) 57:3109–3120
https://doi.org/10.1007/s00603-023-03728-y

ORIGINAL PAPER

A New Analytical Solution for Calculating Rock Block Volume

Gessica Umili[1] · Maria Teresa Carriero[2] · Battista Taboni[1] · Maria Rita Migliazza[2] · Anna Maria Ferrero[1]

Received: 27 July 2023 / Accepted: 12 December 2023 / Published online: 31 January 2024
© The Author(s) 2024

Abstract
The study of rock slope stability and evolution suffers from many uncertainty factors related to block size and shape, and slope morphology. While nothing can be done to remove the aleatory component of these uncertainties, efforts in reducing the epistemic ones are desirable. This research aims to propose a new analytical solution for calculating rock block volume in the case of three discontinuity sets whose orientation and true spacing are known. Researchers and practitioners can take advantage of such a correct analytical formula thanks to its easiness of use: guidelines based on stereogram are provided in order to explain how to obtain the required input data. The correctness of the equation is demonstrated by comparing the results of the new solution applied to 12 theoretical blocks with those obtained with 3DEC (Itasca Consulting Group). Also, the differences with respect to results obtained with the well-known Palmstrøm's formula are reported. The new methodology is applied to the case study of Elva valley road (Northern Italy), which is overhung by steep rocky cliffs and is subject to the consequences of frequent rockfall phenomena. The results are used to discuss the proposed method's applicability: while it is evident that such a formula is not able to compete with the great potentiality of DFNs, this user-friendly tool can quickly and at no cost assess rock block volume in rockfall or rock slope stability studies.

Highlights

- The correct analytical solution for calculating rock block volume is demonstrated.
- The formula is valid in the case of three discontinuity sets.
- Orientation and true spacing of the three sets are the input of the formula.
- Validation is performed through a Discrete Fracture Network generator.

Keywords Block · Volume · Joints · Rock mechanics · Theoretical analysis · Numerical methods

1 Introduction

The intersections among discontinuity planes delimit rock blocks; the shape and orientation of the discontinuities determine whether the block is finite, removable and possibly unstable, and its volume (Goodman and Shi 1985). Estimating the block's volume is not trivial, and many attempts have been made to propose simple analytical methods (Hoek and Bray 1981; Warburton 1981; Palmstrøm, 1996, 2001, 2005). Block volume estimation is fundamental for many different rock engineering applications and, particularly in the study of rockfall phenomena, for the design of barriers in terms of energy absorption capacity and location, where the determination of the so-called "design block" is required (Spadari et al. 2013; Ferrero et al. 2016; Vagnon et al. 2020). In this case, the determination of the design block can be done based on the blocks observed at the slope toe or based on the rock structure determined by geo-structural surveys. The block determination based on measuring the block volumes at the slope toe suffers from a possible major bias error. During their path along the slopes, the blocks can break and reduce their volume significantly, leading to a dangerous

✉ Gessica Umili
gessica.umili@unito.it

[1] Department of Earth Sciences, University of Turin, Via Valperga Caluso 35, 10125 Turin, Italy

[2] Department of Structural, Geotechnical and Building Engineering, Polytechnic of Turin, Corso Duca Degli Abruzzi 24, 10129 Turin, Italy

underestimation (Corominas et al. 2017; Ruiz-Carulla et al. 2017; Giacomini et al. 2009). On the other hand, a method that can compute volumes from discontinuity spacing and orientation is needed if geo-structural data are utilized. In the literature, the first analytical formulations based on geo-structural data date back to the eighties (Hoek and Bray 1981; Warburton 1981). Methods for modeling polyhedral rock blocks with general shapes were then developed, but only in the form of algorithms capable of identifying rock blocks generated from the intersection of discontinuities (Lin et al. 1987; Jing 2000; Lu 2002; Elmouttie et al. 2010). More recently, the advent of the Discrete Fracture Network (DFN) generators made it convenient to generate 3D models of rock mass portions from which to obtain single block volumes (Xu and Dowd 2010; Lambert et al. 2012; Francioni et al. 2020). This research aims instead to propose a new analytical solution for calculating rock block volume in the case of three discontinuity sets whose orientation and true spacing are known. Only the effect of the geometrical properties of the discontinuities within a rock mass is considered, although realistically, slope morphology plays a crucial role in defining detachable blocks. The new formula shall be considered the correct way to calculate the volume delimited by three discontinuity planes, and therefore it should be intended as a fast tool researchers and practitioners can take advantage of, thanks to its easiness of use, while being aware of its limitations with respect to DFN generators. In fact, the average users of the volume analytical formula generally do not have access to sophisticated numerical codes such as DFNs, or to the resources they might require: both economically and in terms of expertise and skill required to use them properly. They usually need a quick method to assess a design block for performing rockfall simulations rather than simulating the structure of an entire rock mass. The results of the new solution applied to 12 theoretical blocks are compared with those obtained from the traditional Palmstrøm's formulation and those produced by a DFN generator, such as 3DEC (Itasca Consulting Group). Finally, the application to the case study of Elva valley road (Northern Italy), which is overhung by steep rocky cliffs and is subject to the consequences of frequent rockfall phenomena, is analyzed to discuss the implications of adopting the proposed method in a real case.

2 State-of-the-Art on Analytical Solutions for Calculating Block Volume

The first attempt to estimate the volume defined by a subdivision of the rock due to discontinuity planes was proposed by Miles (1972). Blocks were assumed to be created either by three discontinuity sets with a negative exponential spacing probability distribution (regular subdivision) or by a random space partition with planes placed by a Poisson process with uniform density (random subdivision) (Ross 2009).

Hoek and Bray (1981) proposed an analytical solution for calculating the volume of a wedge generated by two intersecting discontinuity planes, the upper ground surface, the slope face and, if present, a tension crack. The aim of this calculation is to obtain the weight of the wedge, in order to compute the factor of safety associated with the wedge sliding. The block volume is calculated based on the orientation of the planes, the slope height referred to the first discontinuity plane and, if tension crack exists, its distance from the crest, measured along the trace of the first discontinuity plane. A certain number of calculation steps are required to complete the process. While this procedure is rigorous, it is only suitable for a very specific object such as a wedge, formed by four or five planes. Therefore, for using this procedure in a general case, one must trace everything back to the wedge case, namely associate to each block surface a defined role.

Warburton (1981) proposed a method to perform the vector stability analysis of a rock block in a constrained geometrical configuration. Within the calculation process, one can find a method for calculating areas of block faces, together with the block's volume and center of mass of an arbitrary polyhedral rock block with any number of free faces. However, this method employs the 3D coordinates of the points belonging to the block's edges, which derive from previous calculation steps. Furthermore, the volume is not calculated through an analytical formula: the block is discretized into pyramids whose volume is calculated and summed.

Palmstrøm (1996, 2005) produced simple analytical solutions for estimating block volume from various types of joint density measurements. His well-known equation in the case of three discontinuity sets generating a block is:

$$V_B = \frac{S_1 S_2 S_3}{\sin\gamma_{12}\sin\gamma_{23}\sin\gamma_{13}}, \tag{1}$$

where S_1, S_2, and S_3 are the spacing of the three sets of discontinuities; γ_{12} is the angle between set 1 and set 2, and similarly for γ_{23} and γ_{13}. Equation 1 became a cornerstone in volume estimation, and many academics and professionals adopted it.

Recently, Lopes and Lana (2017) proposed an analytical solution able to overcome the need for measuring mutual angles among sets. The solution is based on linear algebra and vectorial analysis concepts. Volume depends on discontinuity orientations, spacing, and block shape, and the solution is developed for tabular, prismatic, and tetrahedral blocks. Lopes and Lana affirm that a discontinuity plane

with dip ϕ_n, dip direction θ_n, and spacing S_n can be represented by its director vector $\overrightarrow{\mu'_n} = (A_n, B_n, C_n)$, where

$$\begin{bmatrix} A_n \\ B_n \\ C_n \end{bmatrix} = \begin{bmatrix} S_n sin(\phi_n) cos(\theta_n) \\ S_n sin(\phi_n) sin(\theta_n) \\ S_n cos(\phi_n) \end{bmatrix}. \quad (2)$$

They stated that the volume V of a block created by three discontinuity sets could be calculated as:

$$V = \left| \left(\overrightarrow{\mu'_1} \times \overrightarrow{\mu'_2} \right) \cdot \overrightarrow{\mu'_3} \right| = |det(M)|, \quad (3)$$

where

$$M = \begin{bmatrix} A_1 & A_2 & A_3 \\ B_1 & B_2 & B_3 \\ C_1 & C_2 & C_3 \end{bmatrix}.$$

Equation 3 is based on the so-called scalar triple product, namely the dot product of one of the vectors with the cross product of the other two. The absolute value of the scalar triple product represents the parallelepiped volume because, basically, it consists of the product of the area of the basis (calculated by the cross product) for the height (calculated by the dot product). Equation 3 gives the volume of a six-face solid. Still, spatially these direction vectors may also define a solid with a different number of faces; therefore, the result could need to be multiplied by a constant, depending on the actually considered shape of the block.

3 Proposal of a New Formula

Even if the geometrical approach based on the triple product is correct, the solution described by Eq. 3 cannot properly consider true spacing. In fact, considering the definition given by Palmstrøm (2001), the discontinuity set spacing is the normal or minimum distance between individual discontinuities within a discontinuity set. Focusing on the geometrical meaning of the definition, normal set spacing is the distance between a pair of adjacent discontinuities from the same set, perpendicular to the average orientation in that set (Riquelme et al. 2015). From this definition, a new method is proposed in the following.

Considering the coordinate system represented in Fig. 1, the components of the three director vectors $\overrightarrow{\mu_n} = (a_n, b_n, c_n)$ are:

$$\begin{bmatrix} a_n \\ b_n \\ c_n \end{bmatrix} = \begin{bmatrix} S_n sin(\phi_n) sin(\theta_n) \\ S_n sin(\phi_n) cos(\theta_n) \\ S_n cos(\phi_n) \end{bmatrix} n = 1, 2, 3. \quad (4)$$

Then, reasoning about the relation among discontinuity planes is made to understand the role of spacing. Let us consider three discontinuity sets whose director vectors are called $\overrightarrow{\mu_1}, \overrightarrow{\mu_2}, \overrightarrow{\mu_3}$. The cross product of the vectors $\overrightarrow{\mu_1}, \overrightarrow{\mu_2}$ gives the normal $\overrightarrow{m_{12}}$ to both vectors. In the general case, it does not correspond to the normal to the third vector:

$$\overrightarrow{m_{ij}} = \left(\overrightarrow{\mu_i} \times \overrightarrow{\mu_j} \right) \neq \overrightarrow{\mu_k}, \quad (5)$$

considering the three combinations of indices (i, j, k) = (1,2,3), (2,3,1), (3,1,2). Therefore, the spacing of the third set S_3 must not be considered as if it developed along $\overrightarrow{m_{12}}$. Similarly, S_1 and S_2 must not be considered as if they developed along $\overrightarrow{m_{23}}$ and $\overrightarrow{m_{31}}$, respectively. From Eq. 4, it is possible to define spacing as follows:

$$\begin{cases} S_1 = \left\| \overrightarrow{\mu_1} \right\| \\ S_2 = \left\| \overrightarrow{\mu_2} \right\| \\ S_3 = \left\| \overrightarrow{\mu_3} \right\| \end{cases}. \quad (6)$$

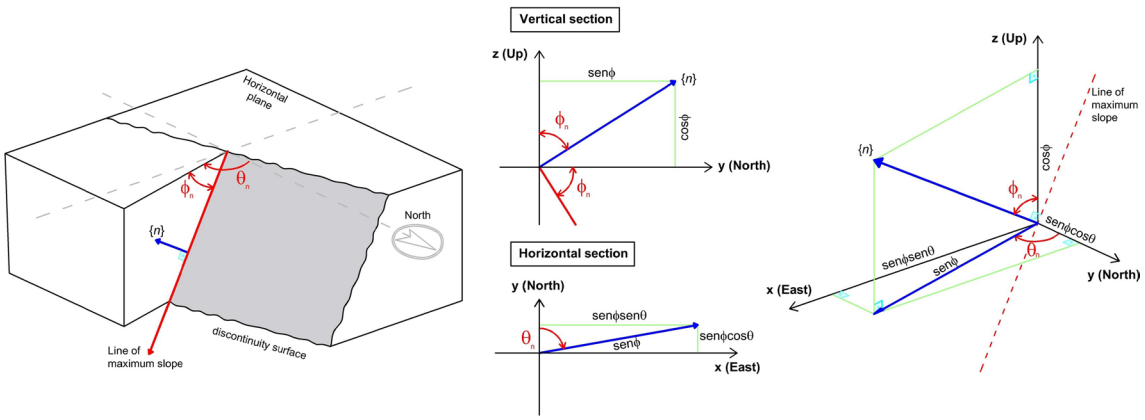

Fig. 1 Coordinate system and discontinuity plane

Following the reasoning, the length of the block's edges is not equal to spacing. In fact, spacing S_k develops along $\overrightarrow{\mu_k}$, while each edge connecting the two faces perpendicular to $\overrightarrow{\mu_k}$ develops along $\overrightarrow{m_{ij}}$.

Therefore, to use spacing values in volume calculation, it is necessary to consider the real direction along with it develops. The orthogonal projection of a vector along the direction $\overrightarrow{\mu_k}$ can be expressed as:

$$\overrightarrow{p_k} = \frac{\overrightarrow{l_{ij}} \cdot \overrightarrow{\mu_k}}{\left\|\overrightarrow{\mu_k}\right\|^2} \overrightarrow{\mu_k}, \tag{7}$$

where

$$\overrightarrow{l_{ij}} = \left(\frac{\overrightarrow{\mu_i}}{\left\|\overrightarrow{\mu_i}\right\|} \times \frac{\overrightarrow{\mu_j}}{\left\|\overrightarrow{\mu_j}\right\|} \right). \tag{8}$$

It is possible to demonstrate that Eq. 7 involves all the three director vectors. Let us call γ_{ij}, γ_{jk}, γ_{ki} the angles between pairs of sets, according to the terminology used by Palmstrom (1996). Moreover, let us call $\delta_{k\text{-}ij}$ the angle between the director vector $\overrightarrow{\mu_k}$ and the direction of the normal to the other two director vectors $\overrightarrow{l_{ij}}$. Similarly, $\delta_{i\text{-}jk}$ is the angle between $\overrightarrow{\mu_i}$ and $\overrightarrow{m_{jk}}$, $\delta_{j\text{-}ki}$ is the angle between $\overrightarrow{\mu_j}$ and $\overrightarrow{m_{ki}}$.

Recalling the definition of cross product, it is possible to write Eq. 8 as:

$$\left\|\overrightarrow{l_{ij}}\right\| = sin\gamma_{ij}. \tag{9}$$

Also, recalling the definition of the dot product, it is possible to explicit the numerator of Eq. 7 as:

$$\overrightarrow{l_{ij}} \cdot \overrightarrow{\mu_k} = \left\|\overrightarrow{l_{ij}}\right\| \left\|\overrightarrow{\mu_k}\right\| cos\delta_{k-ij}. \tag{10}$$

By substituting Eq. 9 in Eq. 10, we obtain:

$$\overrightarrow{l_{ij}} \cdot \overrightarrow{\mu_k} = sin\gamma_{ij} \left\|\overrightarrow{\mu_k}\right\| cos\delta_{k-ij}. \tag{11}$$

Therefore, substituting Eq. 11 in Eq. 7 and reordering factors, we obtain:

$$\overrightarrow{p_k} = \frac{\left\|\overrightarrow{\mu_k}\right\| sin\gamma_{ij} cos\delta_{k-ij}}{\left\|\overrightarrow{\mu_k}\right\|^2} \overrightarrow{\mu_k}, \tag{12}$$

which can be simplified in:

$$\overrightarrow{p_k} = \frac{\overrightarrow{\mu_k}}{\left\|\overrightarrow{\mu_k}\right\|} sin\gamma_{ij} cos\delta_{k-ij}, \tag{13}$$

where $\frac{\overrightarrow{\mu_k}}{\left\|\overrightarrow{\mu_k}\right\|}$ represents the direction of $\overrightarrow{\mu_k}$.

Let us call q_k the norm of $\overrightarrow{p_k}$:

$$q_k = \left\|\overrightarrow{p_k}\right\| = sin\gamma_{ij} cos\delta_{k-ij}. \tag{14}$$

Considering again the three combinations of indices (i, j, k) = (1,2,3), (2,3,1), (3,1,2), which respect the circular shift, one can observe that:

$$sin\gamma_{12} \cos\delta_{3-12} = sin\gamma_{23} \cos\delta_{1-23} = sin\gamma_{31} \cos\delta_{2-31}. \tag{15}$$

Therefore,

$$q_1 = q_2 = q_3 = q. \tag{16}$$

q is a dimensionless number that depends only on the relative orientation of the three joint sets defining the block, namely the angles among director vectors.

The correct volume of the parallelepiped can be calculated as the triple product of vectors as suggested by Lopes and Lana. Still, Eq. 3 must be modified as follows for considering spacing correctly:

$$V = \left| \left(\overrightarrow{\mu_1} \times \frac{\overrightarrow{\mu_2}}{\overrightarrow{p_2}} \right) \cdot \frac{\overrightarrow{\mu_3}}{\overrightarrow{p_3}} \right|. \tag{17}$$

This means that $\overrightarrow{\mu_1}$ is taken as a reference direction, while $\overrightarrow{\mu_2}$ and $\overrightarrow{\mu_3}$ are projected following the considerations made on Eq. 5. Making explicit Eq. 17 and substituting Eq. 14 in Eq. 17, one obtains:

$$V = \left\|\overrightarrow{\mu_1}\right\| \frac{\left\|\overrightarrow{\mu_2}\right\|}{\left|\sin\gamma_{13}\right|\left|\cos\delta_{2-13}\right|} \left|sin\gamma_{12}\right| \frac{\left\|\overrightarrow{\mu_3}\right\|}{\left|\sin\gamma_{12}\right|\left|\cos\delta_{3-12}\right|} \left|cos\delta_{3-12}\right|, \tag{18}$$

which can be simplified as:

$$V = \left\|\overrightarrow{\mu_1}\right\| \frac{\left\|\overrightarrow{\mu_2}\right\| \left\|\overrightarrow{\mu_3}\right\|}{\left|\sin\gamma_{13}\right|\left|\cos\delta_{2-13}\right|}. \tag{19}$$

And can be expressed as follows by substituting Eq. 14 in Eq. 19 and remembering Eq. 6:

$$V = \left\|\overrightarrow{\mu_1}\right\| \frac{\left\|\overrightarrow{\mu_2}\right\| \left\|\overrightarrow{\mu_3}\right\|}{\left|\sin\gamma_{13}\right|\left|\cos\delta_{2-13}\right|} = \frac{S_1 S_2 S_3}{q_2}. \tag{20}$$

Finally, Eq. 19 can be simply expressed as:

$$V = \frac{S_1 S_2 S_3}{q}. \tag{21}$$

Equation 17 can be thus written as:

$$V = \left| \left(\overrightarrow{\mu_1} \times \frac{\overrightarrow{\mu_2}}{\overrightarrow{p_2}} \right) \cdot \frac{\overrightarrow{\mu_3}}{\overrightarrow{p_3}} \right| = \frac{|det(M)|}{q^2}, \tag{22}$$

where

$$M = \begin{bmatrix} S_1\sin(\phi_1)\sin(\theta_1) & S_2\sin(\phi_2)\sin(\theta_2) & S_3\sin(\phi_3)\sin(\theta_3) \\ S_1\sin(\phi_1)\cos(\theta_1) & S_2\sin(\phi_2)\cos(\theta_2) & S_3\sin(\phi_3)\cos(\theta_3) \\ S_1\cos(\phi_1) & S_2\cos(\phi_2) & S_3\cos(\phi_3) \end{bmatrix}.$$

The proposed formula requires input, for each of the three discontinuity sets, true spacing S_n and orientation expressed as dip ϕ_n and dip direction θ_n; q must be calculated as one of the terms of Eq. 15. It is fundamental to remember that the scalar triple product is unchanged under a circular shift of its three operands: the three combinations of indices $(i, j, k)=(1, 2, 3), (2, 3, 1), (3, 1, 2)$, which respect the circular shift, give exactly the same result. In this analytical solution, q represents a non-orthogonality coefficient, while spacing values S_1, S_2, and S_3 represent scale coefficients.

4 Calculation of q

The above demonstrated equations can be practically used to calculate q. Considering Eqs. 14 and 15, it is possible to write:

$$q = sin\gamma_{12}\cos\delta_{3-12} = sin\gamma_{23}\cos\delta_{1-23} = sin\gamma_{31}\cos\delta_{2-31}. \quad (23)$$

Two alternative methods can be used to calculate q: the first one is purely analytical, the second one is based on the stereogram representing the three discontinuity sets orientation. These methods are illustrated in Sects. 4.1 and 4.2, respectively.

4.1 Analytical Calculation of q

In the following, we show how one can simply calculate q based on the orientation and spacing of the three discontinuity planes. The orientation of plane K1 is expressed by dip ϕ_1 and dip direction θ_1, and its spacing is S_1. Similarly, the orientation of plane K2 is defined by dip ϕ_2 and dip direction θ_2, and its spacing is S_2; the orientation of plane K3 is expressed by dip ϕ_3 and dip direction θ_3, and its spacing is S_3.

By replacing these values in Eq. 4, one can write:

$$\overrightarrow{\mu_1} = \begin{bmatrix} S_1\sin(\phi_1)\sin(\theta_1) \\ S_1\sin(\phi_1)\cos(\theta_1) \\ S_1\cos(\phi_1) \end{bmatrix}, \quad (24)$$

$$\overrightarrow{\mu_2} = \begin{bmatrix} S_2\sin(\phi_2)\sin(\theta_2) \\ S_2\sin(\phi_2)\cos(\theta_2) \\ S_2\cos(\phi_2) \end{bmatrix}, \quad (25)$$

$$\overrightarrow{\mu_3} = \begin{bmatrix} S_3\sin(\phi_3)\sin(\theta_3) \\ S_3\sin(\phi_3)\cos(\theta_3) \\ S_3\cos(\phi_3) \end{bmatrix}. \quad (26)$$

Then, the angles γ among the pair of sets can be calculated as follows:

$$\gamma_{12} = \cos^{-1}\left(\frac{\overrightarrow{\mu_1}\cdot\overrightarrow{\mu_2}}{\overrightarrow{\mu_1}\overrightarrow{\mu_2}}\right), \quad (27)$$

$$\gamma_{23} = \cos^{-1}\left(\frac{\overrightarrow{\mu_2}\cdot\overrightarrow{\mu_3}}{\overrightarrow{\mu_2}\overrightarrow{\mu_3}}\right), \quad (28)$$

$$\gamma_{13} = \cos^{-1}\left(\frac{\overrightarrow{\mu_1}\cdot\overrightarrow{\mu_3}}{\overrightarrow{\mu_1}\overrightarrow{\mu_3}}\right). \quad (29)$$

Then, the angles δ among the considered director vector and the direction of the normal to the other two director vectors can be calculated as follows:

$$\delta_{3-12} = \cos^{-1}\left(\frac{\left|\overrightarrow{\mu_3}\cdot\overrightarrow{l_{12}}\right|}{\left\|\overrightarrow{\mu_3}\right\|\left\|\overrightarrow{l_{12}}\right\|}\right), \quad (30)$$

$$\delta_{1-23} = \cos^{-1}\left(\frac{\left|\overrightarrow{\mu_1}\cdot\overrightarrow{l_{23}}\right|}{\left\|\overrightarrow{\mu_1}\right\|\left\|\overrightarrow{l_{23}}\right\|}\right), \quad (31)$$

$$\delta_{2-31} = \cos^{-1}\left(\frac{\left|\overrightarrow{\mu_2}\cdot\overrightarrow{l_{31}}\right|}{\left\|\overrightarrow{\mu_2}\right\|\left\|\overrightarrow{l_{31}}\right\|}\right), \quad (32)$$

where vectors l are calculated according to Eq. 8:

$$\overrightarrow{l_{12}} = \left(\frac{\overrightarrow{\mu_1}}{\left\|\overrightarrow{\mu_1}\right\|}\times\frac{\overrightarrow{\mu_2}}{\left\|\overrightarrow{\mu_2}\right\|}\right), \quad (33)$$

$$\overrightarrow{l_{31}} = \left(\frac{\overrightarrow{\mu_3}}{\left\|\overrightarrow{\mu_3}\right\|}\times\frac{\overrightarrow{\mu_1}}{\left\|\overrightarrow{\mu_1}\right\|}\right), \quad (34)$$

$$\overrightarrow{l_{23}} = \left(\frac{\overrightarrow{\mu_2}}{\left\|\overrightarrow{\mu_2}\right\|}\times\frac{\overrightarrow{\mu_3}}{\left\|\overrightarrow{\mu_3}\right\|}\right). \quad (35)$$

Thanks to the circular shift of the three indices, it is sufficient to calculate only one angle γ and the corresponding angle δ (i.e., Eqs. 27 and 30, or Eqs. 28 and 31, or Eqs. 29 and 32) to solve Eq. 23 and obtain q. The above-listed equations can be easily implemented in a Matlab script to automatize the calculation.

Basically, q is a dimensionless number that depends only on the shape of the block, namely the angles among sets (Umili et al. 2023). The angles γij among sets range between 0° and 180°, while δk-ij range between 0° and 90°: therefore, sine and cosine functions are both limited between 0 and 1. Furthermore, q implies a relative orientation among the sets able to physically produce a closed shape. As a result, q ranges between 0 and 1 with a non-linear trend. If the block

is a regular prism whose angles among sets are all equal to 90°, q is equal to 1. For values of $q < 1$, the volume increases due to the progressively more skewed shape of the block. For $q = 0$, the fraction defining the volume (Eq. 21) is undefined: geometrically, this means that the angle between at least two of the joints is 0°, and they are, therefore, coplanar. In other words, the block is a degenerate polyhedron and infinitely extended. For these reasons, q can be intended as a non-orthogonality coefficient, or rather a polyhedron skewness factor.

Figure 2 shows q values by varying K1 orientation, while the orientation of K2 and K3 is kept constant. In Fig. 2a, the dip of K1 varies between 0° and 90°, the dip direction of K1 varies between 0° and 360°, K2 is 90/090, and K3 is 00/000. As expected, in the cases of perpendicular sets (K1 equal to 90/000, 90/180, and 90/360), q is equal to 1. In Fig. 2b, the dip of K1 varies between 0° and 90°, the dip direction of K1 varies between 0° and 360°, K2 is 61/210, and K3 is 82/100. In Fig. 2c, the dip of K1 varies between 0° and 90°, the dip direction of K1 varies between 0° and 360°, K2 is 53/077, and K3 is 73/185. In Fig. 2d, the dip of K1 varies between 0° and 90°, the dip direction of K1 varies between 0° and 360°, K2 is 66/224, and K3 is 70/307. It is evident that the possible trends of q are many, depending on the relative orientation of the three sets.

4.2 Calculation of q Based on the Stereogram

To illustrate the practical calculation of q, let us consider for example the case in which K1 is 86/180, K2 is 24/185 and K3 is 70/120 (id 5 in Table 1): their orientation can be graphically represented on a stereogram (Fig. 3), on which one can measure the angles required to solve Eq. 23. The first angle required to calculate q is γ_{12}, which is the angle between K1 and K2: it can be measured along the great circle passing through the poles of K1 and K2 (I12 in Fig. 3). In this example γ_{12} is equal to 62.1°. The pole of the plane I12 represents the intersection of planes K1 and K2. The second angle required to calculate q is δ_{3-12}, which is the angle between K3 and I12: it can be measured along the

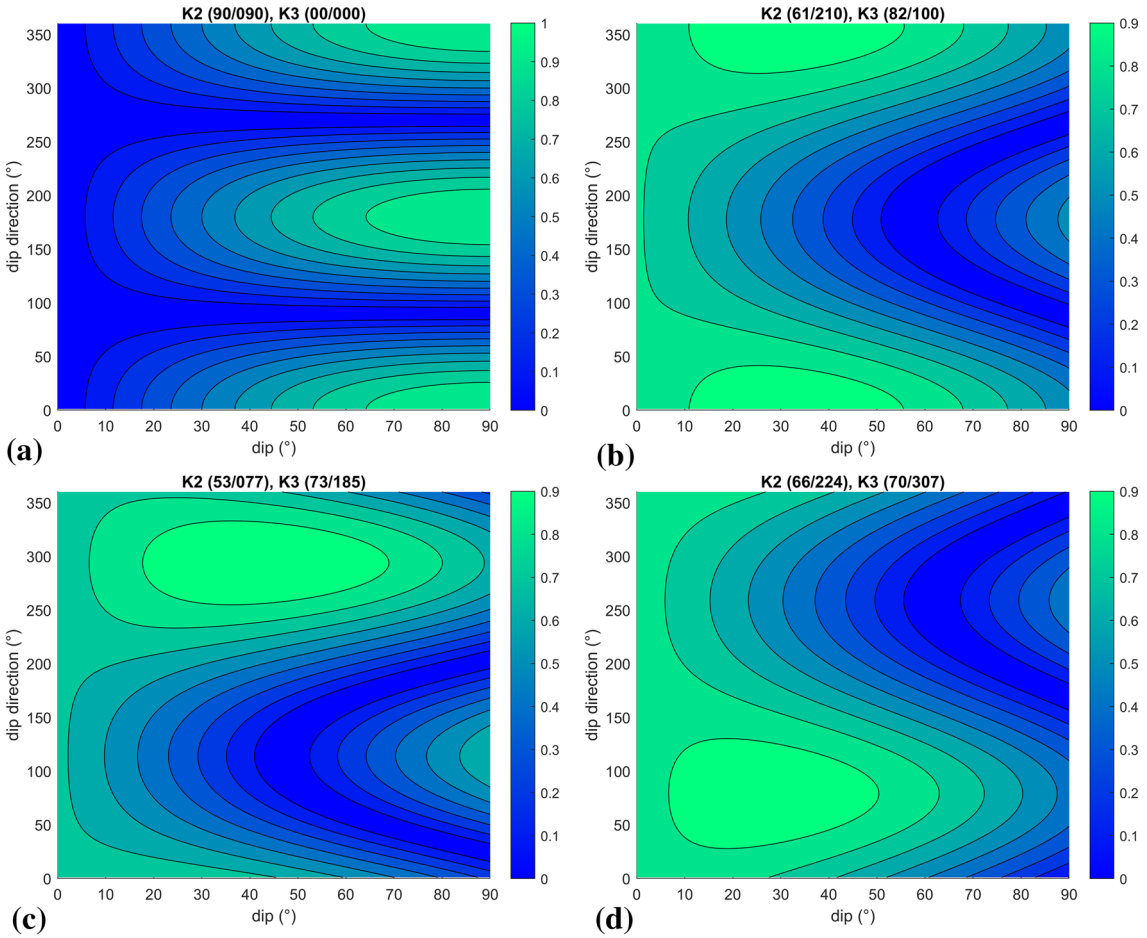

Fig. 2 Values of q by varying dip and dip direction of set K1, while K2 and K3 are kept constant and equal to a) 90/090 and 00/000; b) 61/210 and 82/100; c) 53/077 and 73/185; d) 66/224 and 70/307. The contour step is 0.1

Table 1 Orientation of the three sets considered for the test (unitary spacings), angles, q value and volume V of the block calculated with Eqs. 1 and 21 and 3DEC

Id	K1 [dip/dip dir]	K2 [dip/dip dir]	K3 [dip/dip dir]	γ_{12} [°]	δ_{3-12} [°]	γ_{23} [°]	δ_{1-23} [°]	γ_{31} [°]	δ_{2-31} [°]	q [–]	V Equation 21 [m^3]	V Equation 1 [m^3]	V 3DEC [m^3]
1	90/000	90/090	00/000	90	0	90	0	90	0	1	1	1	1
2	36/352	61/210	82/100	90.74	13.84	93.86	4.20	103.22	13.33	0.9709	1.030	1.030	1.030
3	63/261	53/077	73/185	115.89	20.65	70.19	32.50	93.44	26.52	0.8418	1.188	1.184	1.188
4	15/112	66/224	70/307	72.28	14.17	84.52	17.76	75.89	21.90	0.9236	1.083	1.218	1.083
5	86/180	24/185	70/120	62.10	34.36	60.49	34.05	61.71	33.04	0.7296	1.371	1.477	1.371
6	57/312	44/246	46/112	51.04	23.35	100.87	43.75	81.22	43.37	0.7139	1.401	1.325	1.401
7	35/045	74/277	74/338	96.53	46.64	63.82	36.79	58.40	40.52	0.6821	1.466	1.317	1.466
8	14/301	70/098	35/211	82.96	52.69	37.36	52.91	86.01	7.52	0.6016	1.662	1.664	1.662
9	36/277	52/136	18/049	82.06	55.77	49.62	45.96	53.25	43.00	0.5571	1.795	1.654	1.795
10	52/290	22/084	19/205	72.21	63.58	52.81	43.19	35.53	57.87	0.4237	2.360	2.269	2.360
11	32/120	26/289	33/073	57.71	65.85	24.76	65.31	55.90	34.32	0.3459	2.891	3.411	2.891
12	08/312	15/153	47/079	22.65	45.99	52.11	67.64	44.69	70.19	0.2675	3.738	4.679	3.738

great circle passing through the poles of K3 and I12. In this example δ_{3-12} is equal to 34.36°. By substituting in Eq. 23, q results equal to 0.7296. Proceeding in the same manner, it is possible to measure γ_{23} and δ_{1-23}, which are equal to 60.49° and 34.05°, respectively; similarly, γ_{31} and δ_{2-31} are equal to 61.71° and33.04°, respectively. Inputting these two other pairs of angles the value of q is again equal to 0.7296, as stated in Eq. 23.

5 Verification of the Formula

A cubic model, affected by the presence of three discontinuities sets with orientation reported in Table 1 and spacing equal to 1 m for all the three sets, was generated with 3DEC; null standard deviation was assigned to orientation and spacing values (Fig. 4). As a result, the model contains many blocks generated by the intersection of discontinuities. In general, blocks do not have the same volume. In fact, in close proximity to the model faces, one can find a certain number of smaller blocks produced by the intersection of the discontinuity planes with the boundary surfaces. Representative elementary volume (REV) of the model was investigated to minimize the effect of the smaller blocks on identifying the true block volume. Considering a REV reached if at least 80% of the volume of the blocks falls into the same modal class, a dimension of the virtual rock mass of 35 m was chosen for the following analyses (Carriero et al. 2021). Blocks generated by 12 triples of sets were considered: results of the calculation with the proposed formula (Eq. 21), with Palmstrøm's formula (Eq. 1), and those obtained from 3DEC are reported in Table 1. Cases 1 to 4 are the same used to plot q values in Fig. 2. Then, spacing values were made vary for completing the test: a range between 0 and 3.5 m was considered in order not to change the dimensions of the 3DEC model. Results are reported in Table 2. In all the tests, the perfect agreement of analytical and 3DEC results is obtained, proving the correctness of the proposed solution. Volumes calculated with Palmstrøm's formula show a difference variable from −11% (id = 7) to + 20% (id = 12) with respect to those calculated with Eq. 21.

6 Case Study

The Elva valley road (Northern Italy) is here considered as a case study for discussing the implications of adopting the proposed method. The Elva valley road ("Strada del Vallone" in Italian) is located in the orographic left of the Maira Valley (Piedmont, Northern-western Italy) and directly connects the village of Elva (1637 m a.s.l.) and the Maira Valley. The road stretches for about 9 km along a deep gorge, carved within limestones and dolomitic

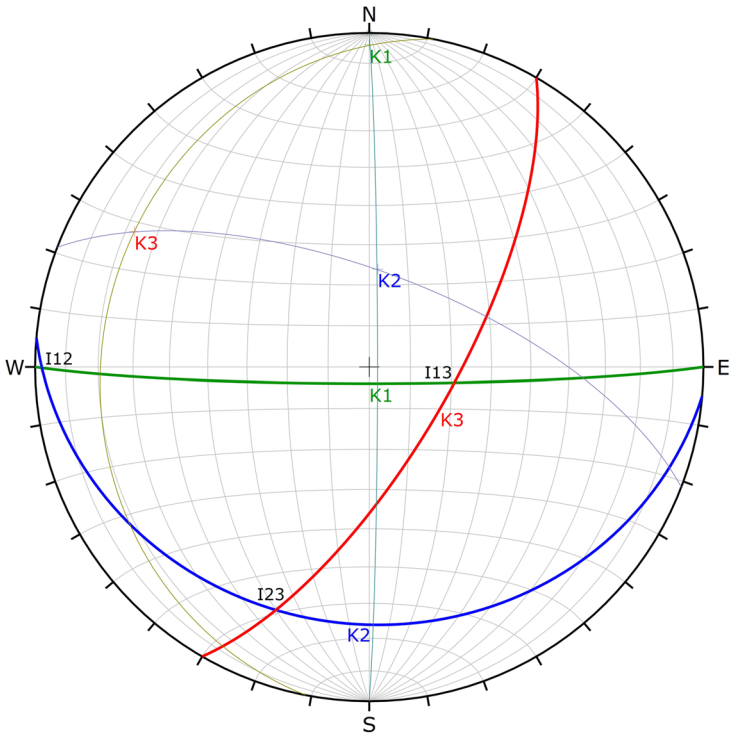

	Color	Dip	Dip Direction	Label
User Planes				
1		86	180	K1
2		24	185	K2
3		70	120	K3
4		88	90	I12
5		67	21	I23
6		21	281	I13

Plot Mode	Pole Vectors
Vector Count	0 (0 Entries)
Intersection Mode	Grid Data Planes
Intersections Count	0
Hemisphere	Lower
Projection	Equal Area

Fig. 3 Calculation of q based on the measurement of angles on a stereogram

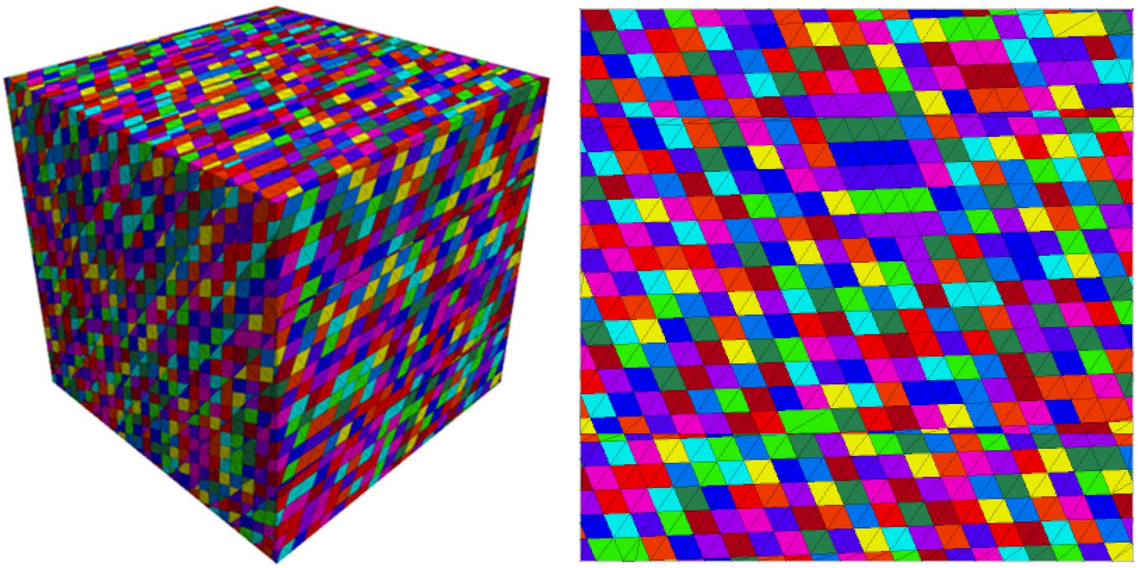

Fig. 4 (Left) Three-dimensional model generated with 3DEC considering the case id 5 (Table 1): K1 86/180; K2 24/185; K3 70/120; (right) detail of one of the model faces

limestones. Steep rocky cliffs overhang almost the entirety of the road: this configuration has produced over the years a large number of rockfall phenomena and rock slides events distributed over a wide area, making it a suitable case study (Fig. 5). Due to the logistical difficulties in assessing the features of the entire rock mass employing direct measures, which can only be used at the road level, non-contact techniques were applied (Migliazza et al. 2021): from the data gathered in this manner, the geometrical features of the rock mass (i.e., orientation and

Table 2 Orientation of the three sets considered for the test, spacing, q value and volume of the block calculated with Eqs. 1 and 21 and 3DEC

Id	K1 [dip/dip dir]	K2 [dip/dip dir]	K3 [dip/dip dir]	S_1 [m]	S_2 [m]	S_3 [m]	q [–]	V Equation 21 [m^3]	V Equation 1 [m^3]	V 3DEC [m^3]
1	90/000	90/090	00/000	0.9	1.1	1.5	1	1.485	1.485	1.485
2	36/352	61/210	82/100	2	1.5	0.7	0.9709	2.163	2.162	2.163
3	63/261	53/077	73/185	1.3	0.5	2.1	0.8418	1.621	1.616	1.621
4	15/112	66/224	70/307	3.2	0.7	1.2	0.9236	2.910	3.273	2.910
5	86/180	24/185	70/120	2	0.8	1.3	0.7296	2.851	3.071	2.851
6	57/312	44/246	46/112	3.1	1.3	0.7	0.7139	3.951	3.738	3.951
7	35/045	74/277	74/338	3.5	2.0	0.4	0.6821	4.105	3.687	4.105
8	14/301	70/098	35/211	0.6	3	0.9	0.6016	2.693	2.696	2.693
9	36/277	52/136	18/049	1.2	0.9	1.3	0.5571	2.520	2.322	2.520
10	52/290	22/084	19/205	0.2	1	1.6	0.4237	0.755	0.726	0.755
11	32/120	26/289	33/073	0.6	1.4	0.5	0.3459	1.214	1.433	1.214
12	08/312	15/153	47/079	0.7	0.7	0.9	0.2675	1.649	2.064	1.649

spacing of the discontinuities) were assessed. Because of the significant length and surface of the rock faces, it became necessary to split the area into sub-domains, where the mechanical and geometrical properties of the rock mass appeared regular enough to be assumed homogeneous (Fig. 6).

In general, the area is characterized by three main discontinuity sets, persistent and identifiable in all the sub-domains: the bedding surface of the limestones (BP) and two conjugated joint sets (K1 and K2). The orientation of the three joint sets changes significantly across the 19 different domains (Table 3). The mean spacing values for the three sets obtained for each sector are reported in Table 4.

For each of the sectors identified in the study area, block volumes were calculated by applying Palmstrøm's formula (Eq. 1). Then, the proposed method for calculating block volume (Eq. 21) was applied, and the results were compared. From the results, visible in Table 4 alongside the input data, it is possible to appreciate how Palmstrøm's formulation is precise and accurate only when the three sets appear to be either orthogonal to each other or very close to orthogonal; in all the other configurations, the block volume can be overestimated (up to 8%) or, more importantly, highly underestimated (up to 56%).

It is interesting to note that if one would choose the global average block volume value as a descriptor of the



Fig. 5 Photographs of the rocky cliffs along the Elva valley road

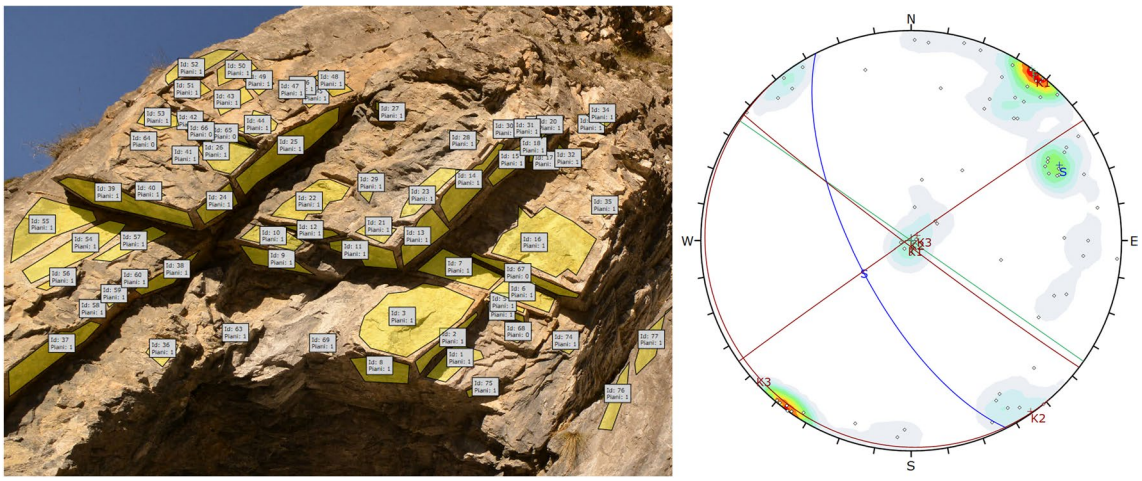

Fig. 6 Non-contact survey of discontinuity orientations and associated stereogram for subarea A2_b

Table 3 Orientation of the three discontinuity sets in the 19 sectors, and calculated angles to be used in Eqs. 1 and 21

Sector	BP [Dip/Dip Dir]	K1 [Dip/Dip Dir]	K2 [Dip/Dip Dir]	γ_{12} [°]	δ_{3-12} [°]	γ_{23} [°]	δ_{1-23} [°]	γ_{31} [°]	δ_{2-31} [°]
B1	70/228	32/073	73/314	99.3	9.5	80.6	9.4	89.9	13.3
B2	33/222	84/257	86/113	57.9	60.8	96.8	65.4	142.7	47.0
B3	28/062	81/293	71/256	98.8	52.8	98.2	52.9	37.2	9.1
B4	28/077	63/299	68/240	84.8	37.7	94.9	37.7	53.4	11.3
B5	19/083	89/124	87/268	74.8	54.0	105.9	53.9	143.8	16.4
B6	35/185	85/197	85/248	50.9	39.7	70.7	50.7	50.8	39.5
B7	24/205	64/078	84/114	79.6	50.4	84.9	51.0	39.7	11.4
B8	43/212	54/330	68/082	80.2	7.9	97.6	10.1	93.5	12.1
A1_a	56/234	61/081	84/200	112.0	48.5	42.1	23.6	111.8	48.6
A1_b	63/261	53/077	73/185	115.9	20.7	70.2	26.5	93.4	32.5
A2_a	68/243	88/217	89/325	32.2	53.5	82.2	71.3	107.9	70.5
A2_b	77/216	88/186	54/064	31.7	35.5	124.3	58.8	114.1	62.1
A2_c	67/092	87/208	90/159	111.6	68.9	68.9	69.0	48.1	63.3
A3_a	69/254	29/086	10/079	97.4	85.1	79.0	85.1	19.1	75.1
A3_b	64/249	87/208	12/078	45.5	25.5	75.9	48.4	94.7	49.7
A4_a	71/281	84/202	88/240	77.7	76.3	43.6	70.3	38.1	67.9
A4_b	66/243	54/195	66/299	42.8	60.1	50.8	64.1	86.5	70.2
A5	60/256	47/068	83/297	106.6	47.5	44.8	23.2	113.1	45.2
A6	86/212	86/338	80/077	125.5	71.7	133.0	69.5	98.1	75.0

general situation along the entire 9 km long road, then by using Eq. 1 that value would be 0.161 m^3; on the other hand, by employing Eq. 21, the global average block volume would be 0.193 m^3. The difference between the two results is in favor of the new equation presented here, as the original formulation provided by Palmstrøm underestimates block volume by 16%. Therefore, the design of any protection work relying on Eq. 1 would provide an undereffective service. The results depicted in Table 4 show that Eq. 1 does not always underestimate block volume, but it is also worth noting that the largest difference between Eq. 1 results and Eq. 21 results (56.6%) is once again an underestimation.

7 Conclusions

A correct calculation method reduces epistemic uncertainty: this is particularly important in studying rockfall phenomena. In fact, when selecting the possible barriers based on their structural capacity of absorbing the design block kinetic energy, it is evident that block volume plays

Table 4 Mean spacing values of the three discontinuity sets in the 19 sectors, values of q and block volumes calculated using Eq. 21, compared to the denominator of Eq. 1, and corresponding volumes obtained by employing Eq. 1

Sector	SBP [m]	S1 [m]	S2 [m]	q [-]	V Equation 21 [m^3]	Denominator of eq, 1 [-]	V Equation 1 [m^3]	ΔV [%]
B1	0.14	0.12	0.16	0.973	0.003	0.974	0.003	−0.1
B2	0.71	0.13	0.43	0.414	0.097	0.510	0.078	−18.9
B3	0.79	0.18	0.54	0.597	0.128	0.591	0.130	1.0
B4	1.05	0.34	0.72	0.788	0.323	0.797	0.320	−1.2
B5	1.08	0.77	0.65	0.567	0.958	0.548	0.990	3.3
B6	1.15	0.48	0.54	0.598	0.499	0.568	0.526	5.3
B7	0.51	0.36	0.42	0.627	0.122	0.626	0.122	0.1
B8	0.22	0.18	0.38	0.976	0.016	0.975	0.016	0.1
A1_a	0.18	0.28	0.17	0.615	0.014	0.577	0.015	6.5
A1_b	0.29	0.27	0.36	0.842	0.034	0.845	0.034	−0.4
A2_a	0.66	0.19	0.37	0.317	0.145	0.503	0.091	−37.0
A2_b	0.47	0.28	0.31	0.428	0.095	0.396	0.102	8.0
A2_c	0.62	0.53	0.68	0.334	0.671	0.645	0.348	−48.2
A3_a	0.23	0.24	0.40	0.084	0.258	0.319	0.068	−73.6
A3_b	0.38	0.46	0.41	0.644	0.114	0.690	0.106	−6.6
A4_a	0.38	0.16	0.36	0.232	0.095	0.416	0.053	−44.2
A4_b	0.23	0.12	0.42	0.338	0.035	0.526	0.022	−35.6
A5	0.17	0.32	0.35	0.648	0.029	0.621	0.031	4.4
A6	0.12	0.20	0.27	0.256	0.026	0.589	0.011	−56.6

a fundamental role, together with the slope morphology. In the case of naturally occurring rock slopes or rock faces, the morphology of the topographic surface is the product of the detachment of unstable portions of the rock mass, i.e., rock blocks. In other words, the rock face morphology is heavily influenced by the geometrical and geomechanical properties of the discontinuities within the rock mass. The formulation introduced in the present work can, in any case, account for the morphology of the slope, as it can be inputted into the equations as any other plane. In fact, the method relies on spacing and orientation of generic geometric surfaces, whatever thei nature. For instance, it is possible to quantify the volume of an unstable rock wedge referring to the geometrical features of the two joints and those of the slope itself. This could be useful also when dealing with artificial slopes, for calculating volumes defined by benches of known orientation and spacing. This research work demonstrates that in the simple case of a rock block generated by three discontinuity sets with known orientation and true spacing, the proposed analytical solution is correct and produces the same value as a DFN code. Moreover, as it has been shown for the case of the Elva valley road, the original Palmstrøm's formula tends to overestimate or underestimate block volume, due to the fact that the assumptions it relays on are true only in the case of three joint sets orthogonal or close to orthogonal among each other. From a practical point of view, an overestimation of the volume, if reasonable, can lead to a more conservative design of protective measures, but an underestimation always represents a significant problem. Therefore, the use of the proposed calculation method of block volume provides a significantly safer approach to the problem.

Moreover, the new method proposed in this paper has an advantage over DFN modeling, which would be the only other methodology providing a correct and precise evaluation of block volume within a rock mass: employing an analytic equation is much simpler, quick, and cheaper than performing DFN modeling. The analytical method to calculate denominator q of Eq. 21 and, most of all, the practical method based on the stereogram, highlight the easiness of use of the formula for calculating the block volume. This point represents a great advantage for practitioners in the sector of rockfall protection works and rock slope stability, who generally need a quick method to assess a design block for performing rockfall simulations, rather than simulating the structure of an entire rock mass through sophisticated and expensive numerical codes such as DFNs.

It must be stated, though, that the new formulation still suffers from the same limitation the Palmstrøm's one had: the equation is valid only in the case of three joint sets; in nature, the likelihood of the occurrence of rock masses with a higher number of discontinuity sets is high, and the new equation cannot address this issue. A possible way to deal with it while still preserving the simplicity of the analytic approach consists in identifying triplets of joint sets and, for each triplet, evaluating block volume; lastly, the relative

importance of each triplet can be estimated by observing niches created by previously detached blocks (Umili et al. 2020) or talus deposits at the toe of the rock face. Otherwise, the construction of a DFN appears as the only feasible way.

Funding Open access funding provided by Università degli Studi di Torino within the CRUI-CARE Agreement. No funding was received for conducting this study.

Declarations

Conflict of interest The authors have no relevant financial or non-financial interests to disclose.

Open Access This article is licensed under a Creative Commons Attribution 4.0 International License, which permits use, sharing, adaptation, distribution and reproduction in any medium or format, as long as you give appropriate credit to the original author(s) and the source, provide a link to the Creative Commons licence, and indicate if changes were made. The images or other third party material in this article are included in the article's Creative Commons licence, unless indicated otherwise in a credit line to the material. If material is not included in the article's Creative Commons licence and your intended use is not permitted by statutory regulation or exceeds the permitted use, you will need to obtain permission directly from the copyright holder. To view a copy of this licence, visit http://creativecommons.org/licenses/by/4.0/.

References

Carriero MT, Ferrero AM, Migliazza MR, Umili G (2021) Comparison between methods for calculating the volume of rock blocks. IOP Conf. Ser.: Earth Environ. Sci. 833:012049. https://doi.org/10.1088/1755-1315/833/1/012049

Corominas J, Mavrouli O, Ruiz-Carulla R (2017) Rockfall Occurrence and Fragmentation. In: Sassa K, Mikoš M, Yin Y (eds) Advancing Culture of Living with Landslides. WLF 2017. Springer, Cham. https://doi.org/10.1007/978-3-319-59469-9_4

Elmouttie M, Poropat G, Krähenbühl G (2010) Polyhedral modelling of rock mass structure. Int J Rock Mech Min Sci Geomech Abstr 47(4):544–552. https://doi.org/10.1016/j.ijrmms.2010.03.002

Ferrero AM, Migliazza MR, Pirulli M et al (2016) Some open issues on rockfall hazard analysis in fractured rock mass: problems and prospects. Rock Mech Rock Eng 49(9):3615–3629. https://doi.org/10.1007/s00603-016-1004-2

Francioni M, Antonaci F, Sciarra N, Robiati C, Coggan J, Stead D, Calamita F (2020) Application of unmanned aerial vehicle data and discrete fracture network models for improved rockfall simulations. Remote Sensing 12:2053. https://doi.org/10.3390/rs12122053

Giacomini A, Buzzi O, Renard B, Giani GP (2009) Experimental studies on fragmentation of rock falls on impact with rock surfaces. Int J Rock Mech Min Sci 46(4):708–715. https://doi.org/10.1016/j.ijrmms.2008.09.007

Goodman E, Shi, Gen-hua (1985) Block theory and its application to rock engineering richard. Berkeley Prentice-Hall, INC., Eng/ewood Cliffs, New Jersey 07632

Hoek E, Bray JW (1981) Rock slope engineering: revised third edition. institution of mining and metallurgy, London. 358 pages

Jing L (2000) Block system construction for three-dimensional discrete element models of fractured rocks. Int J Rock Mech Min Sci 37:645–659. https://doi.org/10.1016/S1365-1609(00)00006-X

Lambert C, Thoeni K, Giacomini A, Casagrande D, Sloan S (2012) Rockfall hazard analysis from discrete fracture network modelling with finite persistence discontinuities. Rock Mech Rock Eng 45:871–884. https://doi.org/10.1007/s00603-012-0250-1

Lin D, Fairhurst C, Starfield AM (1987) Geometrical identification of three-dimensional rock block systems using topological techniques. Int J Rock Mech Min Sci Geomech Abstr 24(6):331–338. https://doi.org/10.1016/0148-9062(87)92254-6

Lopes P, Lana M (2017) Analytical method for calculating the volume of rock blocks using available mapping data field. Math Geosci 49(2):217–229. https://doi.org/10.1007/s11004-016-9635-0

Lu J (2002) Systematic identification of polyhedral rock blocks with arbitrary joints and faults. Comput Geotech 29:49–72. https://doi.org/10.1016/S0266-352X(01)00018-0

Migliazza M, Carriero MT, Lingua A, Pontoglio E, Scavia C (2021) Rock mass characterization by uav and close-range photogrammetry: a multiscale approach applied along the Vallone dell'Elva Road (Italy). Geosciences 11:436. https://doi.org/10.3390/geosciences11110436

Miles RE (1972) The random division of space. Adv Appl Probab 4:243–266. https://doi.org/10.2307/1425985

Palmstrøm A (1996) Characterizing rock masses by the RMi for use in practical rock engineering. Tunn Undergr Space Technol 11(2):175–188. https://doi.org/10.1016/0886-7798(96)00015-6

Palmstrøm A (2005) Measurements of and correlations between block size and rock quality designation (RQD). Tunn Undergr Space Technol 20(4):362–377. https://doi.org/10.1016/j.tust.2005.01.005

Palmstrøm A (2001) Measurement and characterization of rock mass jointing. In: Sharma VM, Saxena KR (Eds.), In Situ Characterization of Rocks. A.A. Balkema Publishers, pp. 49–97

Riquelme AJ, Abellán A, Tomás R (2015) Discontinuity spacing analysis in rock masses using 3D point clouds. Eng Geol 195:185–195. https://doi.org/10.1016/j.enggeo.2015.06.009

Ross SM (2009) Introduction to probability and statistics for engineers and scientists (4th ed.). Associated Press. p. 267. ISBN 978–0–12–370483–2

Ruiz-Carulla R, Corominas J, Mavrouli O (2017) A fractal fragmentation model for rockfalls. Landslides 14:875–889. https://doi.org/10.1007/s10346-016-0773-8

Spadari M et al (2013) Statistical evaluation of rockfall energy ranges for different geological settings of New South Wales, Australia. Eng Geol 158:57–65. https://doi.org/10.1016/j.enggeo.2013.03.007

Umili G, Bonetto S, Mosca P et al (2020) In situ block size distribution aimed at the choice of the design block for rockfall barriers design: a case study along Gardesana road. Geosciences 10(6):223. https://doi.org/10.3390/geosciences10060223

Umili G, Taboni B, Ferrero A (2023) The influence of uncertainties: a focus on block volume and shape assessment aimed at rockfall analysis. J Rock Mech Geotech Eng 15(9):2250–2263. https://doi.org/10.1016/j.jrmge.2023.03.016

Vagnon F et al (2020) Eurocode 7 and rock engineering design: The case of rockfall protection barriers. Geosciences 10(8):1–16. https://doi.org/10.3390/geosciences10080305

Warburton PM (1981) Vector stability analysis of an arbitrary polyhedral rock block with any number of free faces. Int J Rock Mech Mining Sci Geomech Abstracts 18(5):415–427. https://doi.org/10.1016/0148-9062(81)90005-X

Xu C, Dowd P (2010) A new code for discrete fracture network modelling. Comput Geosci 36(3):292–301. https://doi.org/10.1016/j.cageo.2009.05.012

Publisher's Note Springer Nature remains neutral with regard to jurisdictional claims in published maps and institutional affiliations.